Antal Kerpely Doctoral School of Materials Science and Technology
Faculty of Materials Science and Engineering, University of Miskolc

Ecole Doctorale des Sciences de la Matière, du Rayonnement et de l'Environnement
Université Lille Nord de France

Theses

Investigation of Interface Phenomena in Formamide–Water Systems by Computer Simulation Methods

Written by:

Bálint Gábor Kiss

Supervisors:

Dr. Milán Szőri, Prof. Dr. Abdenacer Idrissi and Prof. Dr. Pál Jedlovszky

2020.

1. INTRODUCTION

Mankind has always been fascinated with the mystery of the origin of life. Scientists have been trying for centuries to solve and understand the process of the formation of life as known on our Earth today. In 1938, a new theory in the "The Origin of Life" was published by Oparin.[1] Based on this work, the prebiotic chemical evolution theory was developed. According to the ever-expanding theory of prebiotic evolution, from simple precursors, such as H_2, H_2O, N_2, NH_3, CO, and CO_2, through a complex network of prebiotic chemical reactions under plausible conditions occurred the formation of several building blocks of biomacromolecules, such as nucleotides and amino acids. To confirm this theory, Miller[2] built an apparatus to model the atmosphere of the early Earth, in which CH_4, NH_3, H_2O and H_2 were circulated. His experiment was a success, as he was able to identify different amino acids. During the last decades there has been an increasing amount of both theoretical and experimental evidences suggesting that hydrogen cyanide (HCN) and its hydration product formamide ($HCONH_2$, FA) might have played a key role in the prebiotic evolution. Matthews et al. sketched in their works[3] a HCN based world, where polypeptides and polynucleotides, formed from HCN polymers, were the precursors of both proteins and nucleic acids. Laboratory and extraterrestrial studies suggest that HCN polymerization is a universal process that proceeds in our days as well as in the past in the interstellar medium (ISM) on planetary bodies or even satellites. Hence, we arrived to another significant question: was life born on Earth or somewhere else? The above-mentioned facts suggest the existence of protein-based life in an Earth-like environment also elsewhere in the Universe.

The Swedish chemist Svante Arrhenius proposed the radiopanspermia hypothesis in 1903.[4] According to this, seeds of life travelled by solar radiation to Earth. Oró published in 1961 his hypothesis, according to which comets impacting the primitive Earth could be the source of terrestrial materials, including some important precursors for prebiotic synthesis.[5] Current astrochemical research address the question how prebiotic molecules happened to reach the early Earth, creating the opportunity for the formation of life as we know it, and whether this process could happen elsewhere in the Universe. Many molecules of interest for exobiology have been detected in comets: Comet Hale-Bopp showed hydrogen cyanide, formaldehyde methane, acetylene, formic acid, acetonitrile, hydrogen isocyanide, isocyanic acid, cyanoacetylene, and thioformaldehyde content.[6] These findings indicate that molecules in cometary grains could have played an important role of organic materials reaching the primitive Earth.

Formamide is present in galactic centers,[7] star-forming regions of dense molecular clouds,[8] high-mass young stellar objects,[9] the interstellar medium[10] and comets.[11] Of all the molecules that can be found in space, the frequently detected formamide is one of the most significant one in regard to the prebiotic evolution. High energy particles, heat, electromagnetic radiation, and radioactive decay continuously interact with simple chemical precursors to yield new complex derivatives. If the activated molecule can interact with the proper reactant, then amino acids, nucleobases, sugars, lipids, and carboxylic acids can emerge very easily as synthesizable molecules.[12] Formamide is a key precursor molecule, as it has an amide functional group to form chains of amino acids and build up proteins. It is a precursor of carboxylic acids, amino acids, and sugars, furthermore in the presence of an energy source, it promotes the synthesis of adenine, guanine, cytosine, and uracil, which are the four nucleobases of ribonucleic acid.[13] However, under the extremely low densities present in the interstellar medium, sufficient formamide chemistry requires strong local enhancement of the formamide concentration. Such areas of locally high formamide concentration can again be expected at the surfaces of icy objects, such as cometary[14] or interstellar[15] dust grains that are frequently covered

by low density amorphous ice (LDA). It is important to note that if formamide is formed on solid surfaces, its gas-phase detection and the subsequent (photo)chemistry processes would thus strongly depend on the formamide interaction with water molecules (WAT).[16]

Similarly to water, formamide is also a network-forming liquid,[17] they both form continuous and extensive hydrogen-bonding network. Hence, these molecules can locally substitute each other in the hydrogen bond network, although such substitution may change the topology of the network. Due to these similar properties of the two neat liquids, mixtures of formamide and water are often thought to be examples of the ideal mixture.[18] Indeed, these two compounds are fully miscible with each other,[19] and the thermodynamic properties, such as the energy, entropy and free energy of their mixture depend almost linearly on the composition. The change of the energy and enthalpy occurring upon mixing the two compounds in any proportion turned out to be very close to zero both in experiments[20,21] and in computer simulations.[22]

Neat liquid formamide[23] and its aqueous mixtures[24] have been studied by computer simulation methods on several occasions, due to their aforementioned great importance. However, in simulating liquid mixtures, one has to encounter the problem that potential models that work perfectly for the respective neat liquids might be incompatible with each other, resulting in a poor reproduction of the properties of the mixtures. If the thermodynamic driving force behind the miscibility of the two compounds is small, then limited miscibility of certain model pairs of the two fully miscible compounds may occur.[25] Since the mixing of water and formamide is close to the ideal mixing,[20–22] the thermodynamic changes occurring upon their mixing are expected to be rather small. Consequently, the thermodynamic driving force of this mixing must be small, which makes the above issue – concerning the compatibility of the potential models with each other and their ability to reproduce full miscibility – particularly important for these mixtures.

To the best of our knowledge, no computer simulation study has targeted so far the liquid-vapor interface of formamide-water mixtures as well as ice surfaces containing adsorbed formamide molecules, although the above questions concerning the mixing of these molecules and the fate of formamide in the modern atmosphere as atmospheric pollutant[27] as well as the biomimetic modelling of polypeptides are closely related also to the behavior of formamide at the surface of dense aqueous phases. To contribute to the prebiotic evolution, concentration enrichment of formamide is also essential. These phenomena may take place at interfaces like water or ice in the atmosphere of Earth or in the interstellar medium, as in the case of HCN.[28,29] The detailed understanding of the adsorption of formamide at the surface of crystalline (I_h) ice at tropospheric temperatures (i.e., around 200 K) is important from the point of view of atmospheric chemistry. On the other hand, its adsorption on LDA ice under interstellar conditions is a process of relevance in astrochemistry, with a special importance also in the field of the above discussed prebiotic evolution. However, due to the extreme conditions, experimental investigation of these problems is far from being straightforward.

Computer technology is unstoppably and essentially spreading to all different branches of science. In our days, computer simulation allows us to make models about such complicated systems that was never possible before, and get an insight into their properties at the atomistic level, even in cases when experiments are too dangerous, expensive, difficult, or impossible to perform, such as under the extreme conditions of the interstellar medium. This way, computer simulation methods provide us with the resource to determine macroscopically measurable properties and to interpret macroscopic phenomena based on the knowledge of the microscopic properties of the studied systems. In statistical mechanics, computer simulation is able to provide exact results for problems, while only approximate results are achieved if other, theoretical methods are utilized. Hence, computer simulations can act as numerical experiments

in testing theories. Comparing the results of the simulation with experimental results, on the other hand, provides the opportunity of verifying the models used in the simulation.

1.1. Aim and Objectives

As presented in the introduction, there are still knowledge gaps in the leading theories in connection with the formation of life, including the role of formamide. To reach an effective formamide enrichment which is necessary for playing a role in the biomolecule synthesis, accumulation of formamide molecules has occurred. This can be explained with the sometimes extreme and complex environments including interfaces. The aim of this doctoral dissertation is to interpret the phenomena occurring at interfaces of formamide-water binary systems using computer simulation methods at ambient and cold condition.

To achieve this purpose, first a formamide-water model pair has to be selected to reproduce the real thermodynamic properties of the binary mixtures. Therefore, the thermodynamics of mixing formamide and water are studied by Monte Carlo simulation applying five widely-used formamide and three water models. The performance of the different model combinations considered is evaluated according to their ability to reproduce full miscibility, and by comparing the calculated energy of mixing to the existing experimental data.[20,21] The formamide-water model pair with the best performance will then be applied for simulations in further investigations of this thesis.

Since other prebiotic precursor molecules show enrichment at the interface of their aqueous mixtures[30], the liquid−vapor interface of formamide−water mixtures is promising for accumulation. Hence, the properties of the interface of formamide aqueous mixtures covering the entire composition range from neat water to neat formamide are then investigated by molecular dynamics simulation and surface analysis. The adsorption of formamide in the surface layer, the density profiles, the lateral self-association, orientation and the dynamics of the surface molecules, as well as their lifetime and diffusion at the liquid surface will be the subject of detailed analysis and discussion.

Alternative to the formamide enrichment at vapor/liquid interface of formamide-water mixtures, adsorption of formamide at cold surfaces was investigated which may have importance in the prebiotic evolution, as well as might support panspermia theory. The adsorption of formamide both at the surface of crystalline (I_h) ice (at 200 K) and at the surface of LDA ice (at 200, 100, and 50 K) is simulated by the Grand Canonical Monte Carlo method. The adsorption isotherms, density profile of the adsorption layer, as well as binding energy and surface orientation of the adsorbed molecules that belong to the first molecular layer are investigated and discussed in detail.

2. COMPUTATIONAL METHODS

Regarding the simulation work, first the Monte Carlo simulation carried out to investigate the thermodynamics of mixing of water and formamide with the paring of five different formamide and three widely used water models. The thermodynamic changes during the mixing have been calculated along a thermodynamic cycle (Figure 1). In the method of thermodynamic integration (TI),[31] the difference of the Helmholtz free energies (A) between states X and Y is calculated as an integral along an arbitrarily chosen path connecting the two states:

$$\Delta A = A_{\mathrm{Y}} - A_{\mathrm{X}} = \int_0^1 \left(\frac{\partial A(\lambda)}{\partial \lambda} \right) \mathrm{d}\lambda \qquad (1)$$

where λ is the coupling parameter that describes this path, its value being 0 in state X and 1 in state Y. The non-fictitious state in our case is λ = 1 (T=298 K). Simulations have been performed at six (virtual) temperatures and nine compositions for each model combination and also for the neat systems.

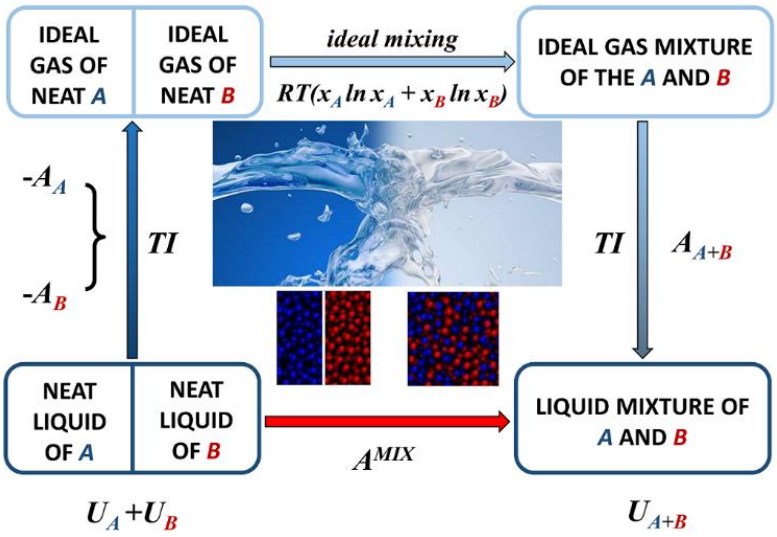

Figure 1: The calculation of the free energy of mixing along a thermodynamic cycle.

The formamide potentials considered include the united atom OPLS model,[32] the all-atom OPLS/AA model[33] modified by Pérez de la Luz et al.[34] (OPLS/AA_mod), the model belonging to the CHARMM force field,[35] and those proposed by Cordeiro[36] and by Macchiagodena et al.[37] (MMPB). For water, we consider the three-site SPC/E[38] and four-site TIP4P[39] and TIP4P/2005[40] potentials. It should be noted that, without additional testing, the CHARMM force field is supposed to be used in combination with the SPC/E, while OPLS with the TIP4P water model. However, the present work represents a far more stringent test of all possible combinations of the above models. All models considered are pairwise additive; the interaction energy of two molecules, *i* and *j*, being within the center-center cut-off distance, is calculated as:

$$u_{ij} = \sum_{\alpha=1}^{N_i} \sum_{\beta=1}^{N_j} \frac{1}{4\pi \in_0} \frac{q_\alpha q_\beta}{r_{i\alpha,j\beta}} + 4\varepsilon_{\alpha\beta}\left[\left(\frac{\sigma_{\alpha\beta}}{r_{i\alpha,j\beta}}\right)^{12} - \left(\frac{\sigma_{\alpha\beta}}{r_{i\alpha,j\beta}}\right)^{6}\right] \qquad (2)$$

Here indices α and β run over the N_i and N_j interaction sites of molecules *i* and *j*, respectively, $\in_0$ is the vacuum permittivity, $r_{i\alpha,j\beta}$ is the distance of site α on molecule *i* from site β on molecule *j*, q_α and q_β are the fractional charges corresponding to the respective interaction sites, while $\varepsilon_{\alpha\beta}$ and $\sigma_{\alpha\beta}$ are the energy and distance parameters, respectively, of the Lennard-Jones interaction of sites α and β, related to the corresponding parameters of the individual sites through the Lorentz-Berthelot rule,[41] i.e., $\varepsilon_{\alpha\beta} = (\varepsilon_\alpha \varepsilon_\beta)^{1/2}$ and $\sigma_{\alpha\beta} = (\sigma_\alpha + \sigma_\beta)/2$.

Molecular dynamics simulations of the liquid-vapor interface of formamide-water mixtures of different compositions, including the two neat systems, have been performed on the canonical (*N*,*V*,*T*) ensemble at the temperature of 300 K. The basic simulation box has contained 4000 molecules. The simulations have been performed at the following mole ratios for FA: 0%, 10%, 20%, 30%, 40%, 50%, 60%, 70%, 80%, 90% and 100%. At the beginning of each simulation, the required number of water and formamide molecules have been placed in a basic simulation box the edges *Y* and *Z* of which have been 50 Å, while the length of the *X* edge has roughly corresponded to the density of the liquid phase. After proper energy minimization,

these bulk liquid systems have been equilibrated. Then the *X* edge of the basic box has been increased to 300 Å, resulting in a system containing the liquid-vapor interface. All results have been averaged over the two liquid-vapor interfaces present in the basic box. The intrinsic surface of the liquid phase has been determined on the sample configurations by the ITIM method.[42] In the ITIM analysis, a probe sphere of the radius of 1.25 Å has been moved along test lines parallel with the *X* edge of the basic box, arranged in a 125 × 125 grid.

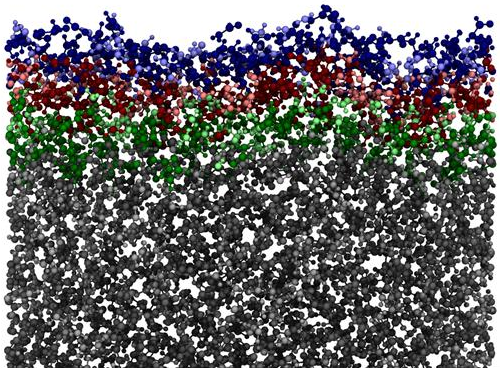

Figure 2: Equilibrium snapshot of the 50% FA system (X > 0 Å half of the basic box). The first (blue), second (red) and third (green) molecular layer. The bulk phase represented by grey color

The adsorption of formamide at the surface of both I_h and LDA ice has been simulated on the grand canonical (μ,V,T) ensemble by the GCMC method. Simulations involving amorphous ice have been performed at the temperatures of 50, 100, and 200 K, while adsorption on I_h ice has only been simulated at 200 K. To obtain the adsorption isotherms, with each adsorbent and every temperature a set of GCMC simulations have been performed in which the chemical potential, μ, of formamide has been systematically varied. The number of the adsorbed formamide molecules has then been determined as a function of the chemical potential. The X, Y, and Z edges of the rectangular basic simulation box have been 100 Å, 35.926 Å, and 38.891 Å, respectively, axis X being perpendicular to the macroscopic plane of the ice surface. We have identified the first layer formamide molecules adsorbed at the surface of amorphous ice using the ITIM method. The first layer formamide molecules identified this way are also indicated in Figure 3.

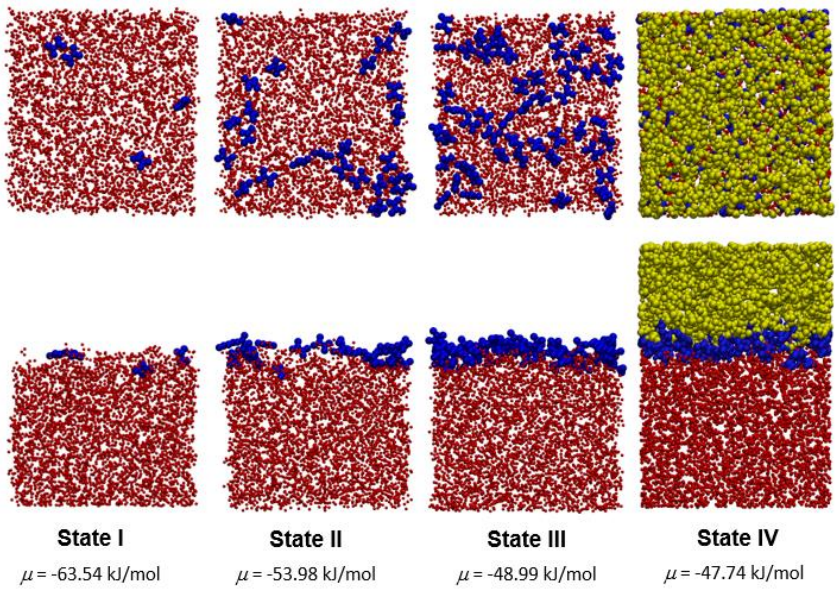

Figure 3: Equilibrium snapshots of the system at 50K, both from top (top line) and side (bottom line) views, as obtained at four different chemical potential values from our simulations. Water molecules (red), first layer formamide molecules (blue) and outer formamide molecules (yellow).

3. RESULTS

3.1. Miscibility and Thermodynamics of Mixing of Different Models of Formamide and Water

To obtain an appropriate model pair, what is able to reproduce the experimental properties of the formamide-water binary system, the chosen force fields which describe formamide (OPLS, OPLS/AA_mod, CHARMM, Cordeiro and MMPB) and water (SPC/E, TIP4P and TIP4P/2005) systems have to be compatible with each other. To test these model pairs, the Helmholtz free energy (A), energy (U), and entropy (S) change accompanying the mixing of neat liquid in formamide-water systems have been calculated. including the two neat systems. These results plotted in Figure 4. The free energy of mixing is negative in every case, indicating that the mixture is always thermodynamically more stable than the two separate neat liquids (Figure 4.a). The magnitude of A^{mix} is rather small, being always below 2 kJ/mol. For comparison, the value of RT is about 2.5 kJ/mol at 298 K. Similarly, small values are obtained for U^{mix} and S^{mix} in every case, their values being always within $RT/2$ and R, respectively. As a consequence, the obtained A^{mix}, U^{mix}, and S^{mix} values are also rather close to each other as obtained with different model combinations, their difference never exceeds 1.3 kJ/mol, 1.8 kJ/mol, and 3.5 J/mol K, respectively.

The energy of mixing (Figure 4.b) shows a qualitatively different behavior in the case of OPLS/AA_mod model compared to other FA models. It is always below zero in mixtures of the OPLS/AA_mod model, but it is positive in all other cases. Although the deviation from the experimental values[20,21] is roughly of the same magnitude with all formamide models considered, the experimental data supports the qualitative behavior of the OPLS, CHARMM, Cordeiro, and MMPB models rather than that of OPLS/AA_mod in this respect. Thus, according to the experimental data,[20,21] the observed negative free energy of mixing of water and formamide is of entropic origin, as the energy of mixing is very small and positive. Consistently, the entropy of mixing is found to be positive for all model combinations.

Figure 4.c also includes the entropy change corresponding to ideal mixing. The obtained S^{mix} values are rather close to this ideal term (shown as dotted line); their difference never exceeds 2.5 J/mol K, and, considering the OPLS, Cordeiro, and MMPB models, this difference always remains below 1 J/molK, being within the error bars of the calculation. Both the energy and entropy of mixing values turned out to be very close to the term corresponding to ideal mixing (i.e., 0 for U^{mix} and $-R[x_{FA}\ln x_{FA} + (1-x_{FA})\ln(1-x_{FA})]$ for S^{mix}) for every model combination and at every composition. Based on the nearly linear dependence the Helmholtz free energy, energy, and entropy of the liquid phase on x_{FA}, the mixing of these to compounds is nearly ideal.

The negative value of A^{mix} is a necessary but not sufficient condition of miscibility; the two components are fully miscible with each other, if the value of the D parameter in the following inequality is positive in the entire composition range:

$$D = 1 + x_A\, x_B \frac{\partial^2 \left(A^{ex} / RT \right)}{\partial x_A^{\,2}} > 0 \qquad (3)$$

To determine the $D(x_{FA})$ data for the different model combinations, instead of numerical second derivative of the A^{ex}/RT, we fitted the Margules equation:[43]

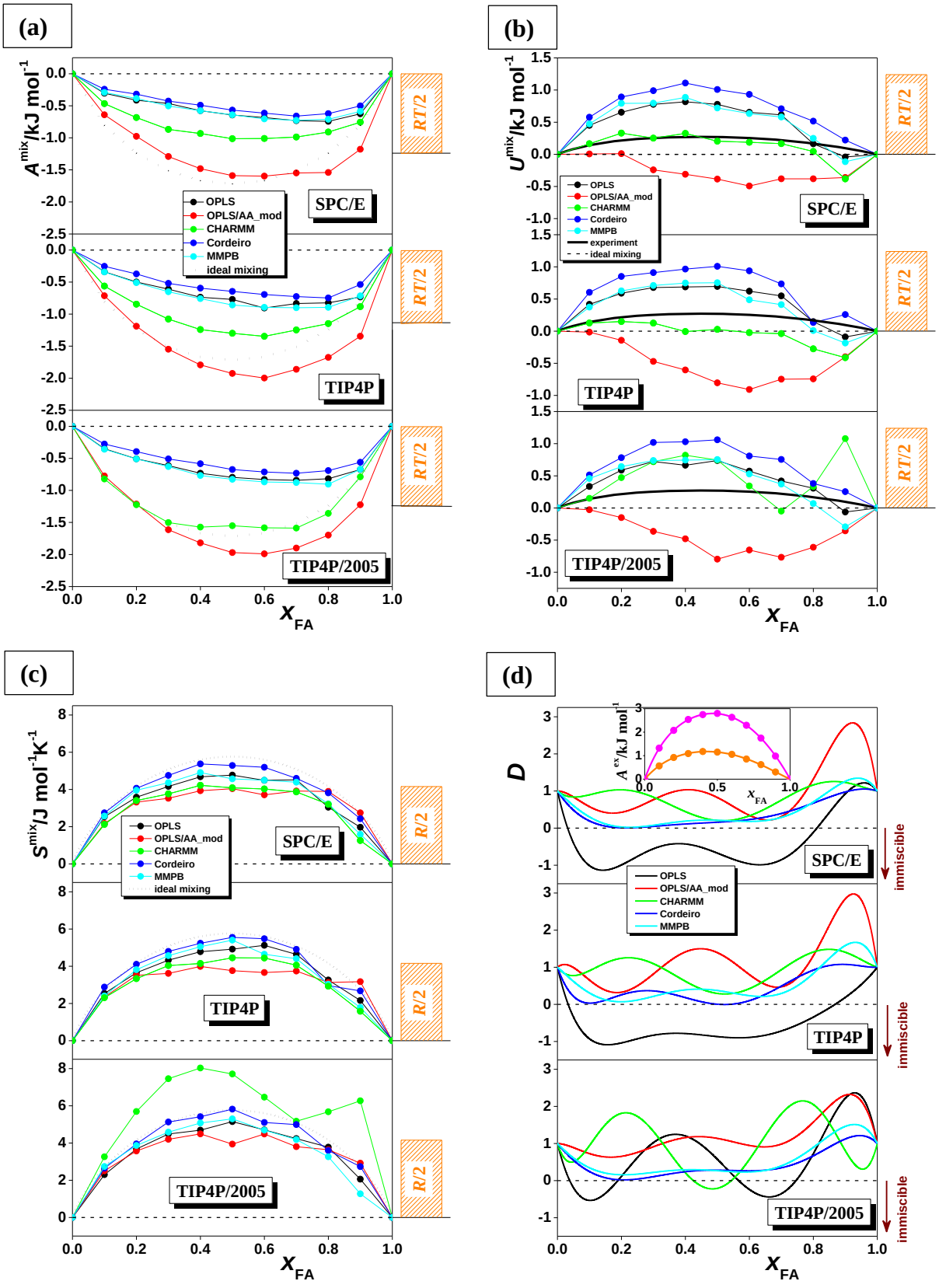

Figure 4: Helmholtz free energy of mixing (a), energy of mixing (b), entropy of mixing (c) and composition dependence of the parameter D (d) of the SPC/E (top panel), TIP4P (middle panel), and TIP4P/2005 (bottom panel) models of water with the OPLS (black), OPLS/AA_mod (red), CHARMM (green), Cordeiro (dark blue), and MMPB (light blue) models of formamide. Zero value is indicated by dashed line and the Helmholtz free energy of ideal mixing is shown by dotted line in diagram (a). Experimental data of the energy of mixing[20,21] is shown by a thick line in diagram (b), the entropy of ideal mixing is shown by dotted line in diagram (c). The average kinetic energy of the molecules along one degree of freedom of RT/2 is also shown for reference by orange bars. The inset (d) shows the calculated A^{ex} data (full circles), together with their Margules fit for mixtures of the OPLS/AA_mod model of formamide with the SPC/E (orange) and TIP4P/2005 (magenta) water models.

The $D(x_{FA})$ curves obtained with the different model combinations considered are shown in Figure 4.d. As is seen from the figure, the OPLS model of formamide shows immiscibility with all of the water models. Further, the $D(x_{FA})$ curves obtained using the Cordeiro and MMPB formamide models in combination with any of the three water models considered are very close to zero. Further, full miscibility of these model combinations might also depend on the details of the simulation (e.g., long range correction, the use of rigid model, etc.). The D values obtained using the OPLS/AA_mod formamide model with any of the three water models considered remains safely above zero in the entire composition range, indicating that the OPLS/AA_mod model is indeed fully miscible with all these three water models. On the other hand, as it has been pointed out previously, these model combinations are qualitatively incompatible with existing experimental data[20,21] in respect to the energy of mixing. The CHARMM and TIP4P/2005 models exhibit a narrow miscibility gap in the x_{FA} range of about 0.4-0.55, while the CHARMM model of formamide is fully miscible with both the SPC/E and TIP4P water models. Further, as seen from Figure 4.b, these model combinations are also qualitatively compatible with the experimental data[20,21] concerning the sign of the energy of mixing. Considering also the fact that the experimental energy of mixing data is somewhat better reproduced when the SPC/E rather than the TIP4P model of water is used, the CHARMM model of formamide had been selected in combination with the SPC/E water model for the subsequent investigations.

3.2 Liquid−Vapor Interface of Formamide−Water Mixtures

After the section of the model pair that best describes the mixing properties of formamide and water, the molecular dynamics simulations of the liquid-vapor interface of formamide-water mixtures of different compositions were performed using this model combination. As is seen, not only the mass density profiles change smoothly between the liquid and vapor phase, but the number density profiles of both molecules also show rather little structure at the interface, apart from a tiny peak occurring at the liquid side of the interface on the formamide density profiles in the systems of low formamide mole fraction (Figure 5). Hence, formamide does not show considerable adsorption at the surface of its aqueous solutions.

The density profiles of the individual molecular layers beneath the liquid surface can be very well fitted by Gaussian functions (Figure 5. bottom panel). The width of these Gaussians, σ, can serve as an estimate of the width of the corresponding layer. The σ values obtained in the first, second, and third molecular layer beneath the surface in the various systems (denoted by σ_{L1}, σ_{L2}, and σ_{L3}, respectively) are summarized in Table 1. It is seen that upon approaching the interface the σ values become smaller, indicating that the corresponding molecular layers get progressively more compact. Thus, the second and third layers are 3-5% and 5-10% thicker than the first layer in every case. This finding is suggests the presence of a strong hydrogen-bonding network in the surface layer, which can partly compensate the energy loss of the surface molecules due to the vicinity of the vapor phase, and which makes the surface layer unusually compact.

To further analyze the arrangement of the surface molecules around each other, we investigated the possibility of their lateral microscopic self-association within the surface layer. For this purpose, we have projected the centers-of-mass of the surface layer molecules to the macroscopic plane of the interface, *YZ*, and calculated the area distribution of the Voronoi cells of these projections. In a two-dimensional set of seeds, the Voronoi cell of a given seed is the locus of the points in the plane that are closer to this seed than to any other one.[44] If the seeds are evenly distributed in the plane, the area of their Voronoi cells, *A*, follows a gamma distribution,[45] i.e.,

$$P(A) = a\, A^{\nu-1} \exp(-\nu\rho A)\,. \qquad (4)$$

In this equation, ν and ρ are free parameters, while the factor a normalizes this probability distribution to unity. If the seeds show considerable self-association, leaving large empty areas between them, the Voronoi cells of the seeds located at the boundary of these empty domains are considerably larger than those being inside the self-associates. As a consequence, the corresponding $P(A)$ distribution deviates considerably from eq. 4, exhibiting a long, exponentially decaying tail at large area values.[46] The Figure 6. shows the $P(A)$ distribution, when one component is disregarded, the resulting distribution is broader than that obtained by considering both components, and gets progressively broader with increasing mole fraction of the disregarded component. More importantly, the $P(A)$ distributions obtained by considering only one of the components can always be reasonable well fitted by eq. 4. Yet, slight deviations of the simulated data from eq. 4. is only seen at large A values in the systems of low FA concentration, indicating that no considerable self-association of the like molecules occurs even within the surface layer. In other words, water and FA molecules turn out to be miscible with each other on the molecular scale even at the surface of their mixtures. This behavior of FA is in accordance with the claim that the mixing of FA with water is nearly ideal.[18,26,47]

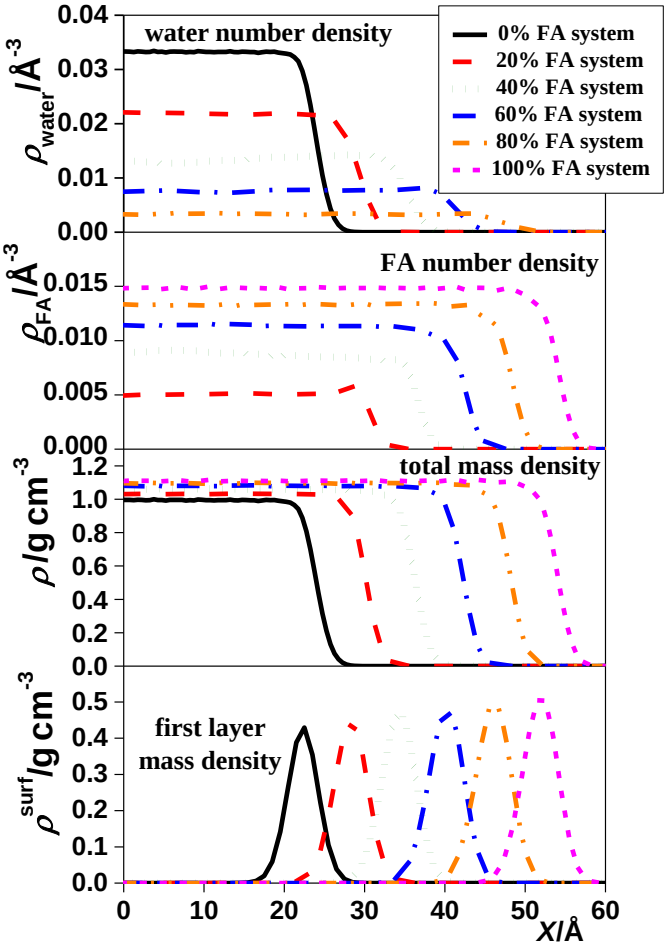

Figure 5: Number density profile of the water (top panel) and formamide (second panel) molecules as well as the mass density profile of the entire system (third panel) and of the surface layer of the liquid phase (bottom panel) along the interface normal axis, X. All profiles shown are averaged over the two interfaces present in the basic simulation box.

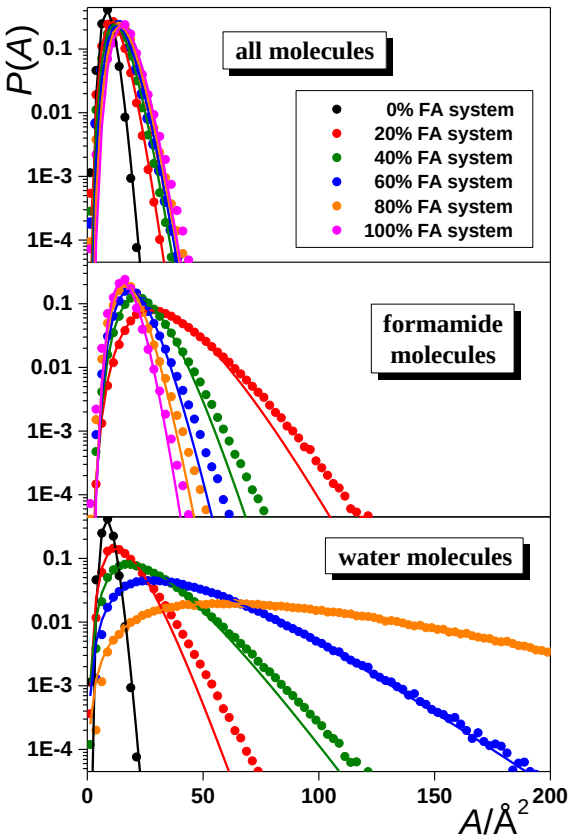

Figure 6: Area distribution of the Voronoi polygons corresponding to the projections of the surface molecules to the macroscopic plane of the surface; all surface molecules (top panel); formamide molecules (middle panel), water molecules (bottom panel). Solid lines show the best fit to the simulation data according to eq. 4.

Table 1: Various Properties of the Systems Simulated[a]

system	σ_{L1}/Å	σ_{L2}/Å	σ_{L3}/Å	τ_{surf}/ps		τ_D/ps		$D_{\|}$/Å^{2}ps^{-1}	
				water	FA	water	FA	water	FA
0% FA	3.79			12.5	-	8.0	-	0.547	-
10% FA	3.97	4.08	4.22	11.3	67.8	11.7	13.3	0.448	0.393
20% FA	4.08	4.27	4.46	11.1	59.8	13.6	15.8	0.422	0.366
30% FA	4.15	4.37	4.55	11.1	55.0	14.9	17.9	0.412	0.345
40% FA	4.20	4.42	4.59	11.3	53.1	17.8	19.1	0.360	0.336
50% FA	4.27	4.50	4.63	11.3	51.0	17.8	20.3	0.376	0.331
60% FA	4.28	4.50	4.61	11.0	49.9	19.8	21.6	0.353	0.323
70% FA	4.31	4.52	4.61	11.3	49.2	20.3	22.3	0.356	0.324
80% FA	4.32	4.54	4.60	11.6	48.9	19.7	24.0	0.380	0.312
90% FA	4.42	4.61	4.66	11.3	48.9	18.8	24.4	0.408	0.316
100% FA	4.34			-	48.9	-	26.0	-	0.307

[a]Error bars affect the last shown decimal digit.

The full description of a rigid molecule relative to an external plane requires two independent orientational variables in our case the $\cos\vartheta$ and ϕ. Therefore, the full description of the orientational statistics can only be done through the bivariate joint distribution of these two variables.[48,49] In order to analyze the orientational distribution relative to the macroscopic plane of the liquid surface, *YZ*, here we define the local Cartesian frames as illustrated in Figure 7.a. Furthermore, to investigate also the effect of the local curvature of the liquid surface on the preferred orientations, we have also calculated the $P(\cos\vartheta,\phi)$ orientational distributions, besides the entire surface layer, also in its separate regions A, B, and C (Figure 7.b). These regions are defined through the mass density profile of the surface layer as follows. Region B covers the *X* range in which the density of the surface layer exceeds half of its maximum value, while regions C and A cover the *X* ranges located closer to and farther from the bulk liquid phase, respectively. The preferred orientations, obtained from the orientational distribution denoted as I_w (for water) and I_{FA} (for formamide) and illustrated in Figure 7.c, correspond to the parallel alignment of the respective molecules with the macroscopic plane of the surface, *YZ*. The observed preferential alignment of both molecules with the macroscopic plane of the surface enables them to form a strong hydrogen-bonding network at the liquid surface.

Both molecules prefer somewhat different orientations at the tips of the crests (region A) and in the bottom of the troughs (region C), i.e., at the strongly positively and negatively curved portions, respectively, of the molecularly rough liquid surface. The water molecule is tilted from the parallel alignment with the *YZ* plane, and points towards the bulk liquid phase (in orientation I_w^A) and towards the vapor phase (in orientation I_w^C) with its H atoms (Figure 7.c). Further, in region A the preferred orientation of the FA molecules, marked here as II_{FA}, is tilted somewhat from the *YZ* plane, pointing with the CHO group to the vapor, and with the NH_2 group to the liquid phase. In region C, the corresponding orientation, marked here as III_{FA}, is perpendicular to the macroscopic plane of the surface, and the NH_2 group points straight to the vapor phase (Figure 7.c). Possible hydrogen bonding patterns of neighboring surface FA and water molecules, both aligned in one of their preferred orientations, and their relation with the local curvature of the molecularly rough surface are illustrated in Figure 7.d.

To investigate the dynamics of the molecules within the surface layer, we have calculated their survival probability and mean residence time as well as their lateral diffusion coefficient, $D_{||}$, within the surface layer (Table 1). The survival probability, $L(t)$, is defined as the probability that a molecule that belongs to the surface layer at t_0 will stay in this layer up to t_0+t. The mean surface residence time values, τ_{surf}, are collected in Table 1. for both molecules. As is seen, formamide molecules stay considerably, i.e., 4-6 times longer at the liquid surface

than waters. Further, while the mean surface residence time of the water molecules does not show any apparent composition dependence, the τ_{surf} value of FA clearly decreases with increasing formamide concentration, being about 30% smaller at the surface of neat formamide than in the 10% FA system. This finding indicates that the presence of water stabilizes the stay of the formamide molecules at the surface of the liquid phase of their mixtures.

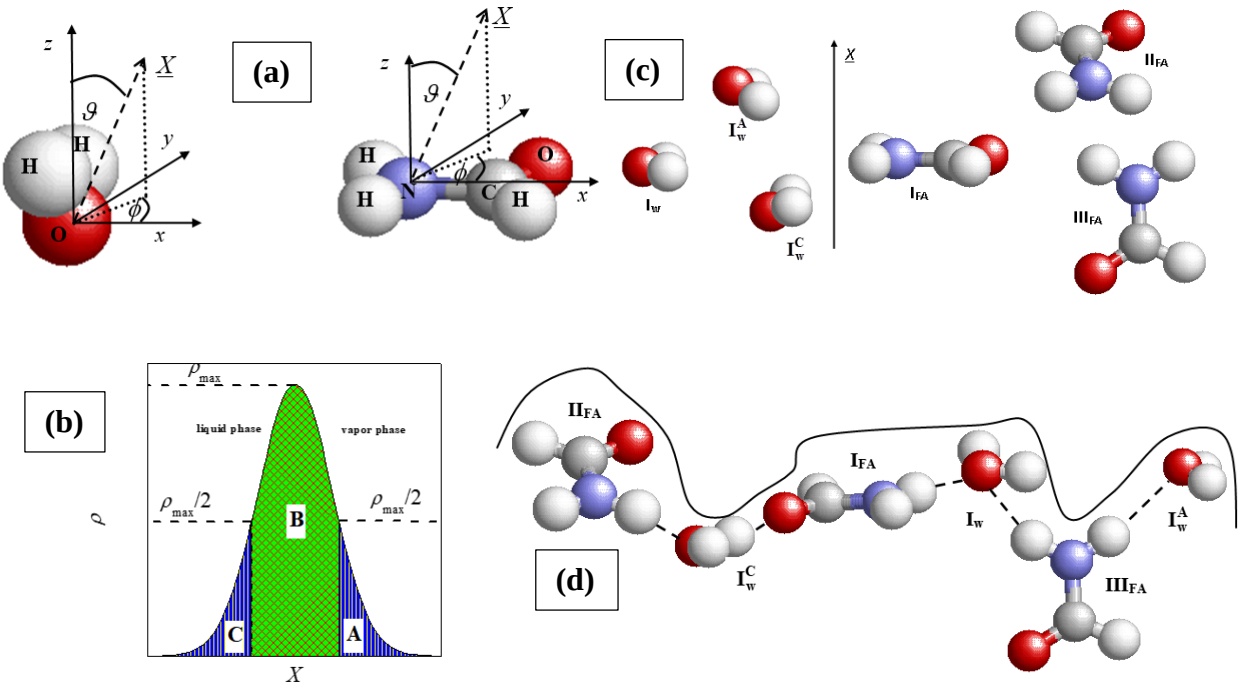

Figure 7: (a) Definition of the local Cartesian frames fixed to the individual water (left) and formamide (right) molecules. (b) definition of the regions A, B, and C of the surface layer. (c) Illustration of the orientations preferred by the water and formamide molecules in the entire surface layer as well as in any of its separate regions A, B, and C, relative to the surface normal vector (pointing, by our convention, towards the vapor phase), X. (d) Illustration of possible hydrogen bonding alignments of water and formamide molecules, both oriented according to their preferences, in portions of different local curvatures of the surface layer. The solid curved is a schematic representation of the liquid surface.

The diffusion time, $\tau_{D,}$ of the molecules within the surface, obtained for the water and FA molecules in the different systems simulated are also included in Table 1. As is seen, for water, τ_{surf} is larger than τ_D only at the surface of the neat system; these two time scales are roughly equal in the 10% FA system, while in the systems of higher formamide concentration the lateral diffusion of the water molecules clearly occur on a larger time scale than their mean surface residence time, indicating that water molecules typically leave the surface of these systems before they could make considerable diffusion there. Since the mean surface residence time of the water molecules is insensitive to the composition of the system, the reason for this behavior is the increase of τ_D with increasing formamide concentration. In other words, our finding indicates that formamide molecules stabilize the water molecules at their position in the surface during the entire time scale of their stay at the surface of such mixtures. It is also seen that, for formamide, τ_{surf} is always noticeably, i.e., by a factor of 2-5 larger than τ_D, indicating that formamide molecules do diffuse at the liquid surface of their aqueous mixtures. The lateral surface diffusion coefficient of formamide is rather insensitive to the composition, as it only exhibits a slight decrease in the entire composition range with increasing FA mole fraction. It is also seen that the surface diffusion of the FA molecules is considerably slower in their

aqueous mixtures than that of the water molecules at the surface of neat water, i.e., where they do exhibit a noticeable diffusion at the liquid surface.

These findings, in the absence of large self-association of the formamide molecules at the surface at any composition, mean from the prebiotic evolutionary point of view that under the examined conditions the enrichment of formamide is not significant at the surface of its aqueous solution. Therefore, its participation in biomolecular synthesis at the vapor-liquid interface of formamide-water systems is not justified.

3.3 Adsorption of Formamide at the Surface of Amorphous and Crystalline Ices under Interstellar and Tropospheric Conditions.

Another important area concerning the investigation of this binary system, beside the liquid-vapor interface, is the adsorption of formamide at various ice surfaces. The adsorption isotherms obtained from the Monte Carlo simulations are shown in Figure 8.a. in the form of number of adsorbed formamide molecules as a function of their chemical potential. As is seen, the isotherm obtained on I_h ice rises continuously up to the chemical potential value of about −60 kJ/mol. This rising part is followed by a plateau in the μ range of about −60 to −57 kJ/mol, corresponding to an adsorption monolayer. This monolayer is rather stable, as evidenced by the fact that it exists in an about 3 kJ/mol wide range of chemical potentials. The plateau is followed by a very steeply rising part of the isotherm, corresponding to multilayer adsorption. This steeply rising part of the isotherm ends at the chemical potential value of about −56 kJ/mol, where the basic box becomes filled with formamide molecules. The plateau observed between −60 and −57 kJ/mol on I_h ice is missing on LDA ice. This finding suggests that the corrugated geometry of the LDA surface promotes multilayer adsorption. As a consequence, multilayer adsorption on LDA starts at μ values at which the adsorbed monolayer is still stable on I_h ice. The shape of the $\langle N \rangle$ (μ) isotherm does not change noticeably with the temperature; it is simply shifted to higher chemical potential values as the temperature decreases.

In order to further analyze the adsorption isotherms, we have converted them to the more conventional Γ vs. p_{rel} form. The obtained $\Gamma(p_{rel})$ isotherms are shown in Figure 8.b. As is seen, at 200 K, the isotherms start rising almost linearly; this rise gradually decreases turning into a plateau, and the plateau part is followed by a second, steeply rising part of the isotherms. The first rising part corresponds to the gradual building up of the first molecular layer; the plateau reflects the presence of a more or less saturated monolayer, while the second, steeply rising part corresponds to multilayer adsorption. At lower temperatures, the plateau of the isotherm gets progressively shorter and occurs at lower surface densities, suggesting that multilayer adsorption starts before the complete saturation of the first molecular layer. Thus, the obtained isotherms represent a transition between type II and type III isotherms (both describing multilayer adsorption) according to the IUPAC convention. Considering that type II isotherms correspond to systems where the adsorbate−adsorbent interaction is considerably stronger, while type III isotherms correspond to systems where it is considerably weaker than the lateral interaction between the adsorbed molecules, this result is in a clear accordance with earlier claims[47] and with our previous findings that the mixing of water and formamide is nearly ideal, and hence there is no marked difference between the interactions of the like and unlike molecules. Furthermore, it is also seen that the steepness of the first, rising part of the isotherm, corresponding to the building up of the first molecular layer, increases very strongly with decreasing temperature, which results in a very sharp rise of the low temperature isotherms even at extremely low p_{rel} values.

On the basis of the behavior of the obtained isotherms, we have selected four chemical potential values in each system, at which sample configurations have been collected for detailed analyses. The lowest of these chemical potential (state I) always corresponds to only a few adsorbed molecules per surface. At the second μ value chosen (state II), formamide molecules form an unsaturated monolayer but cannot be isolated from each other, while at the third μ value (state III) they form a more or less saturated monolayer. Finally, the largest of the chosen chemical potential values (state IV) corresponds to multilayer adsorption in every case. The chemical potential values corresponding to these states are indicated in Figure 3.

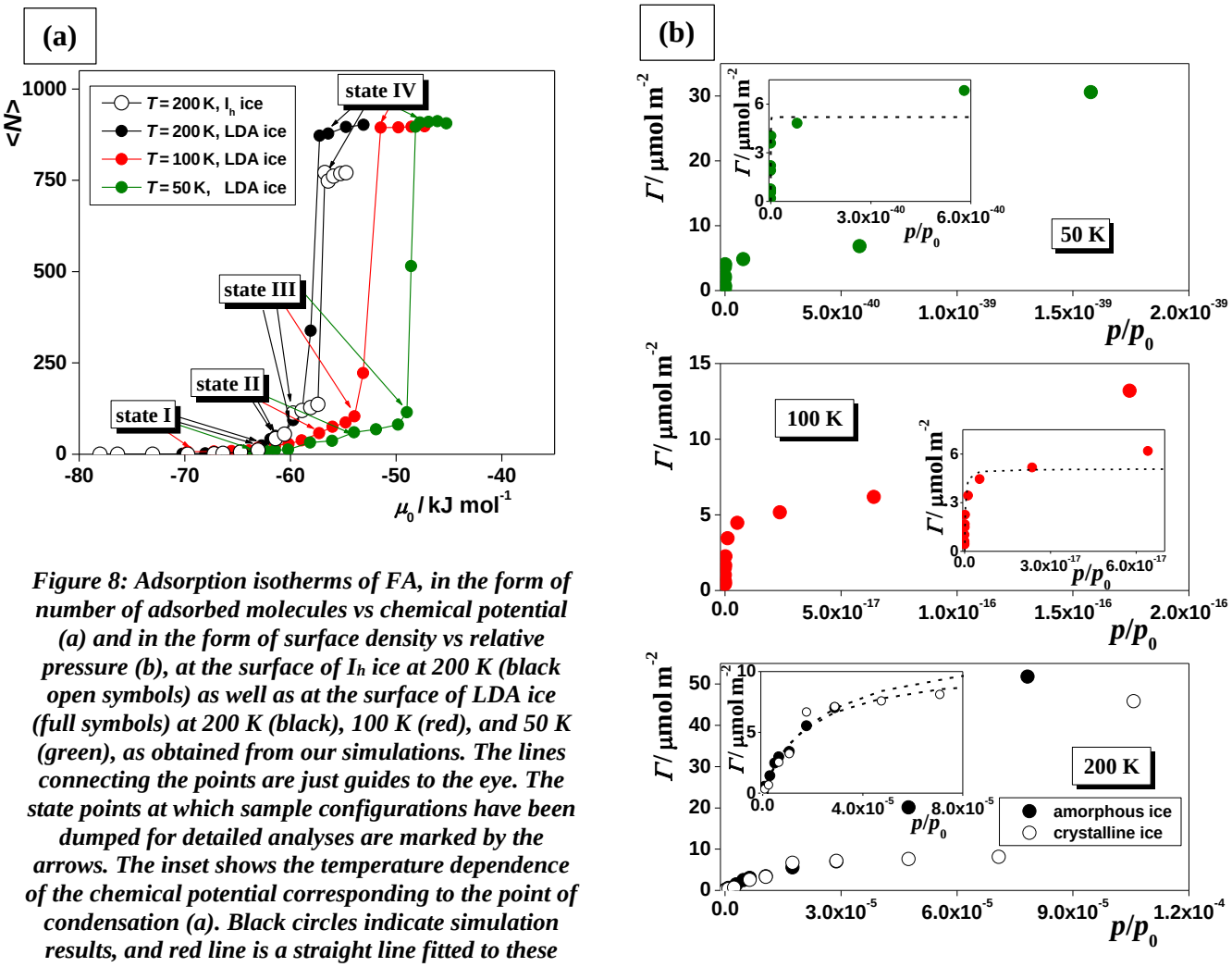

Figure 8: Adsorption isotherms of FA, in the form of number of adsorbed molecules vs chemical potential (a) and in the form of surface density vs relative pressure (b), at the surface of I_h ice at 200 K (black open symbols) as well as at the surface of LDA ice (full symbols) at 200 K (black), 100 K (red), and 50 K (green), as obtained from our simulations. The lines connecting the points are just guides to the eye. The state points at which sample configurations have been dumped for detailed analyses are marked by the arrows. The inset shows the temperature dependence of the chemical potential corresponding to the point of condensation (a). Black circles indicate simulation results, and red line is a straight line fitted to these data. The insets of diagram (b) show these data up to the point where the adsorption layer is still monomolecular (symbols), together with their best Langmuir fits (dashed curves).

The mass density profiles of all formamide molecules as well as of only those forming the first molecular layer at the ice surface along the surface normal axis, X, are shown in Figure 9, as calculated in states I−IV in the various systems considered. The obtained profiles show no substantial amount of formamide is located in the vapor and in the bulk ice phase. For reference, the mass density profile corresponding to the outmost portion of the ice phase is also indicated. It is also seen that the ordered structure of I_h ice implies also a clear layering of the adsorbed formamide molecules in the case of multilayer adsorption, while this layering is effectively screened by the corrugated surface of LDA ice. The comparison of the profiles corresponding

to all formamide molecules and to only those belonging to the first molecular layer reveals that not even traces of multilayer adsorption occur in states I−III. Further, since the saturated adsorption monolayer can be very well estimated by the first molecular layer in state IV, it is also evident that the adsorption monolayer in state III is clearly not yet saturated in any case (see also Figure 3). Since state III has always been chosen as the point immediately preceding the sharp rise of the isotherm, this finding is in a clear accordance with our earlier claim that multilayer adsorption starts before the first monolayer gets saturated.

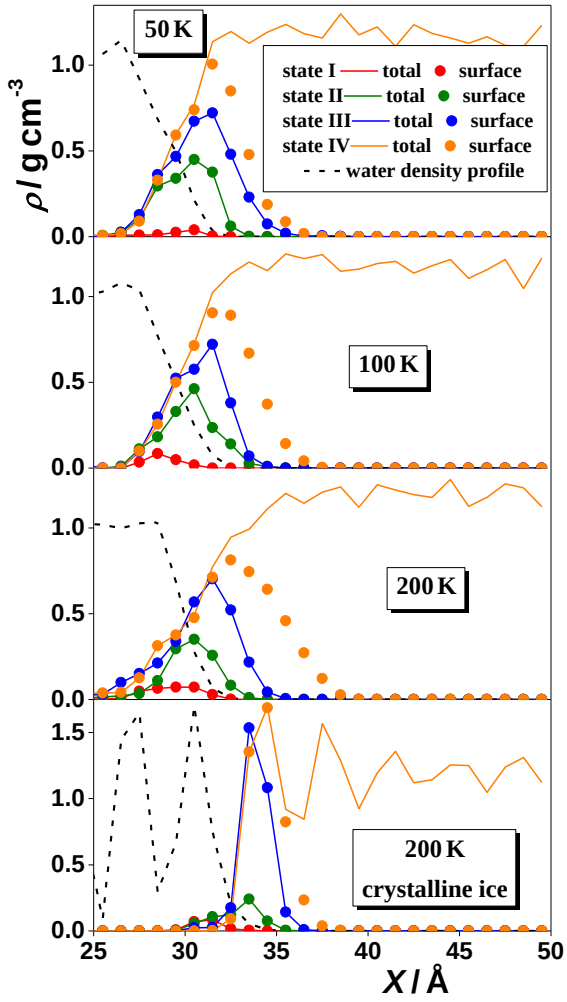

Figure 9: Mass density profile of the adsorbed formamide molecules (solid lines) as well as solely of their first molecular layer (circles) in states I (red), II (green), III (blue), and IV (orange). LDA ice at 50 K (top panel), 100 K (second panel), and 200 K (third panel); I_h ice at 200 K (bottom panel).

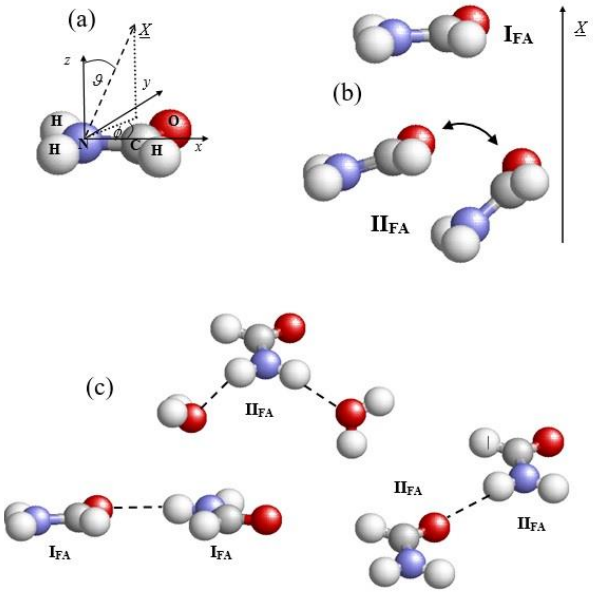

Figure 10: (a) Definition of the local Cartesian frame. (b) Preferred orientations of the formamide molecules at the surface of I_h and LDA ices. (c) Possible H-bonding arrangements of the surface formamide molecules with their formamide neighbors as well as with surface water molecules. The dashed lines denote hydrogen bonding, and X is the macroscopic surface normal

The orientational preferences of the formamide molecules have been determined the similar way then in the case of the liquid-vapor interface. The preferred alignments I_{FA} and II_{FA} of the formamide molecules are illustrated again in Figure 10. The preference of the formamide molecules for these orientations can be understood by considering the possible hydrogen bonds they can form with each other as well as with the surface water molecules in these alignments. Since all the hydrogen-bonding directions of the formamide molecule lay also within the molecular plane, formamide molecules of alignment I_{FA} can easily hydrogen-bond to each other; a formamide molecule of orientation I_{FA} can form up to four such hydrogen-bonds with its formamide neighbors. Further, since the surface of LDA ice is corrugated on the molecular

length scale, two neighboring surface formamide molecules of alignment II_{FA}, located at different depths along the macroscopic surface normal axis, X, can also form a hydrogen-bond with each other in such a way that the molecule being farther from the bulk ice phase along this external axis is the hydrogen-donor, while the one being closer to the bulk ice phase is the hydrogen-acceptor partner. These possible hydrogen bonds between two surface formamide molecules, both aligned in one of their preferred orientations, are illustrated in Figure 10.c.

A formamide molecule of orientation I_{FA}, laying also parallel with this plane, can thus easily form up to four hydrogen-bonds also with surface waters of this alignment. Moreover, even at the surface of I_h ice, a slight deviation from the alignment I_{FA} as well as from a preferred water orientation and/or a slight distortion of the linearity of the hydrogen-bond can also lead to the formation of several hydrogen-bonds between surface waters and I_{FA} aligned formamides. Furthermore, a formamide molecule of alignment II_{FA}, being tilted from the surface plane, can easily donate both of its NH_2 hydrogen atoms to surface water molecules aligned in two of their preferred orientations. These possible hydrogen-bonding patterns between surface water and first layer formamide molecules are also illustrated in Figure10.c.

To characterize the energetic background of the adsorption, we have calculated the U_b binding energy of the first layer formamide molecules. Further, besides U_b, its contributions coming from the interaction with the ice phase and with the other formamide molecules, denoted here as U_b^{ice} and U_b^{lat}, respectively, have also been calculated. The binding energy distributions obtained at 200, 100, and 50 K are shown in the Figure 11.a, b and c respectively. In state I, the $P(U_b^{ice})$ distribution of the 200 K systems exhibits a single peak around −100 kJ/mol. With increasing chemical potential, this peak shifts to higher energies, often being split into two distinct peaks or exhibiting a shoulder. These peaks and shoulders typically occur around the energy values of about −75 kJ/mol, −50 kJ/mol, and −25 kJ/mol, in the case of state IV and I_h ice even a small peak of $P(U_b^{ice})$ around zero energy is seen. Considering that the energy of a hydrogen bond is roughly −25 kJ/mol, this finding indicates that in state I, first layer formamide molecules typically form four hydrogen-bonds with the ice phase, and the number of their hydrogen-bonded water neighbors gradually decreases with increasing surface density. The $P(U_b^{lat})$ distribution exhibits a very high and narrow peak at zero energy in state I; this peak is still clearly seen in state II, and traces of it exist even in state III. This peak corresponds to the adsorbed formamide molecules that are isolated from each other. Interestingly, this distribution also shows a peak at around −25 kJ/mol even in state I on LDA ice, indicating that adsorbed molecules are not completely isolated from each other even in this state of very low surface density. This behavior stresses the strong lateral interaction between the adsorbed formamide molecules. It should be noted that, by contrast with the LDA ice, no such peak is seen on $P(U_b^{lat})$ in state I of I_h ice, indicating that in this case the adsorbed molecules are indeed isolated from each other. The distribution of the total binding energy, $P(U_b)$, exhibits a single peak around −100 kJ/mol in states I−III, reflecting the compensation of the decrease of its ice, and increase of its lateral component with increasing chemical potential, and indicating that adsorbed formamide molecules always prefer to form four hydrogen bonds with their neighbors, irrespective of whether they are waters or formamides. Interestingly, in state IV the $P(U_b)$ peak occurs around −120 kJ/mol. This deep binding energy reflects a strong but non-hydrogen bonding interaction of the first layer formamide molecules with those Fa molecules which are forming the subsequent molecular layers. Considering that first layer formamides already complete their four possible hydrogen-bonds with surface waters and in-layer formamides in the lack of outer adsorbed molecular layers, we can conclude that this interaction

with the subsequent layers in state IV most likely involves strong dipolar interactions, as without that the additional, roughly −20 kJ/mol of the binding energy could not be explained.

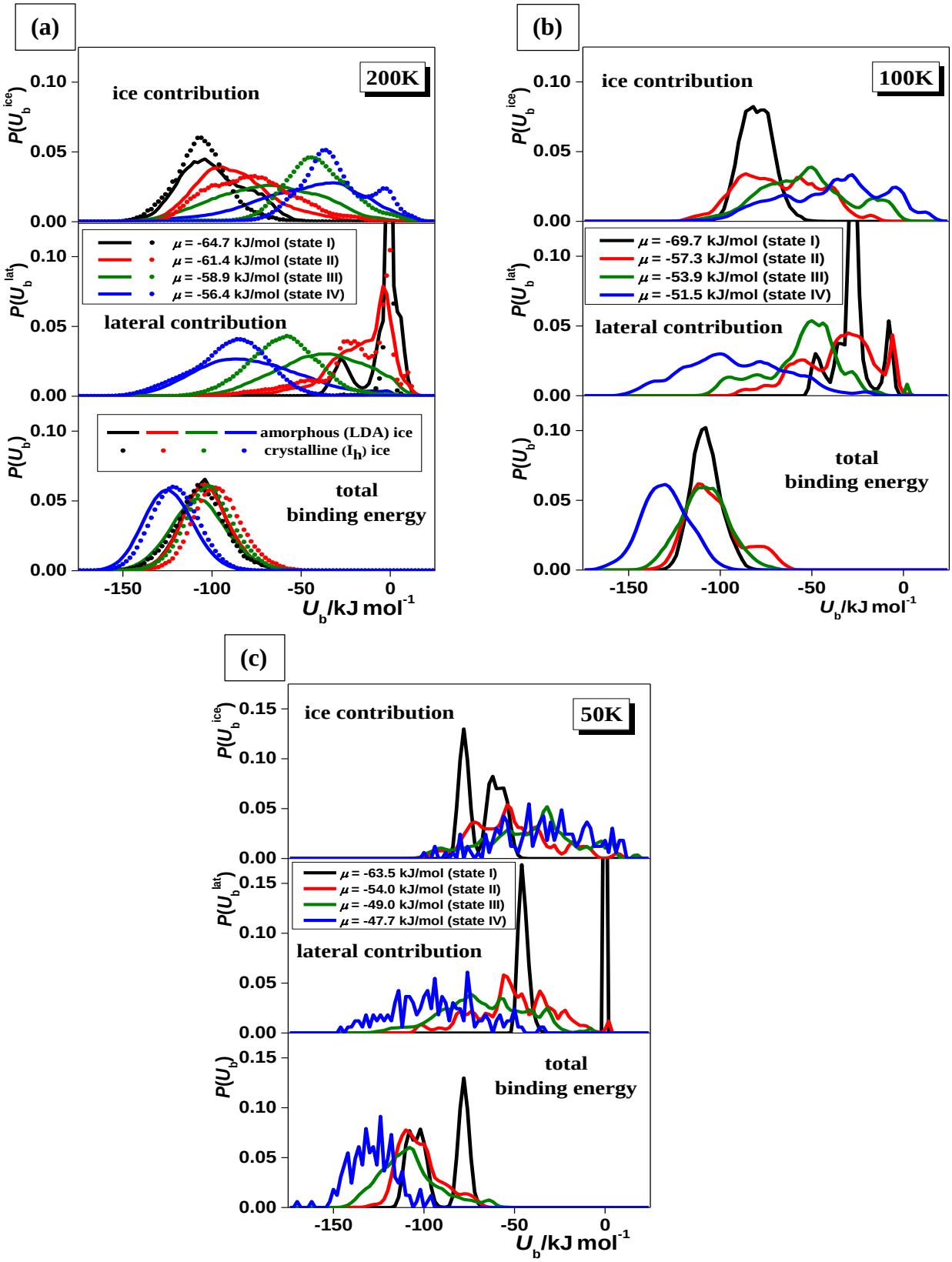

Figure 11: Distribution of the total binding energy (U_b) of the first layer formamide molecules (bottom panels) as well as its contribution coming from the other formamide molecules in the system (middle panels) and from the ice phase (top panels), as obtained at 200 K (a), 100 K (b) and 50 K (c) at the surface of I_h (full circles) and LDA (solid lines) ices in states I (black), II (red), III (green), and IV (blue).

The distributions obtained at lower temperatures indicate that at these low temperatures adsorbed formamide molecules are not at all isolated from each other even at very low surface densities, they are very strongly interacting with each. This extremely strong affinity of the formamide molecules for lateral interaction is in a clear accordance with the observed at the adsorption isotherms, as discussed previously.

These results support the possible role of formamide in the prebiotic evolution theory by suggesting the surface of ice grains in the Earth's atmosphere as a possible location of formamide enrichment. The atmosphere of the early and modern Earth could have thus a possible place of the synthesis of complex biomolecules. Furthermore, due to the adsorption of formamide on the LDA ice surface in the interstellar medium, the synthesis of new complex biomolecules could also occur outside the Earth if initiated by high energy particles (e.g., heat, electromagnetic radiation, etc.). Thus, these observations fit both into the prebiotic and the panspermia hypotheses.

Conclusions in this work presented the possible locations of biomolecule synthesis due to the thick adsorption layer of formamide. However, the "how" is still not fully clarified. Studies in both experimental and computational chemistry have already been published exploring possible reaction pathways in the synthesis with the help of formamide. Based on the identified locations, the range of possible interactions and catalysts can be further narrowed. The results of this thesis also show the importance of hydrogen bonds in the formation of surface phenomena. These secondary bonds proved to be determining in terms of energy and orientation properties of the surface molecules. Hence emphasizes the importance of hydrogen bonds in the formation of life. This raises further questions about what other effects they provide and what role can hydrogen bonds play in the synthesis of biomolecules. Furthermore, hydrogen bonds could promote the formation of asymmetric structures in life-essential macromolecules.

4. Thesis Points

1. I compared the possible combinations of five formamide and three water models by Monte Carlo simulation and thermodynamic integration. Based on the miscibility of the components and the thermodynamic properties, such as the Helmholtz free energy, energy and entropy of their mixing, the most realistic representation of the formamide-water system is found to be the pair of the CHARMM formamide and SPC/E water models.

2. I found the existence of an extensive, percolating hydrogen bonding network at the liquid-vapor interface of formamide-water mixtures, in which the components are interchangeable with each other and the molecules show full miscibility on the molecular level. No strong adsorption or lateral self-association of any of the two components have been detected at the surface layer. Furthermore, formamide molecules have been found to prevent water from considerable diffusion at the liquid surface, while waters have been found to stabilize the stay of the formamide molecules at the surface of their liquid mixtures.

3. I showed that formamide and water molecules prefer parallel alignment with the macroscopic surface plane at the surface of their liquid mixtures. These preferences can be interpreted as the intention to minimize their free energy, hence they are oriented in such a way that the number of hydrogen-bonds they form is maximized.

4. I found that the adsorption of formamide on the surface of crystalline and low-density amorphous ices at atmospheric and interstellar conditions is a strongly favorable phenomenon, which thus leads to a strong enhancement of the formamide concentration. Adsorbed formamide molecules are not isolated from each other on such icy surfaces, in addition, multilayer adsorption begins before the first layer becomes saturated. Based on these findings, the adsorbate-adsorbent and lateral interactions turn out to be of rather similar strengths.

5. I determined the orientational preferences of the adsorbed formamide molecules in the first molecular layer at the surface of crystalline and low-density amorphous ices, which show parallel and tilted alignments relative to the ice surface. Similar to the vapor-liquid interface, formamide molecules try to minimize their free energy in such a way that they form the maximum possible hydrogen-bonds with their neighbors.

Publications Included in The Thesis

1. Miscibility and Thermodynamics of Mixing of Different Models of Formamide and Water in Computer Simulation; B. Kiss, B. Fábián, A. Idrissi, M. Szőri and P. Jedlovszky; *J. Phys. Chem. B* 2017, 121, 7147−7155; *DOI: 10.1021/acs.jpcb.7b04965; Erratum: DOI: 10.1021/acs.jpcb.7b09210*

2. Investigation of the Liquid−Vapor Interface of Water−Formamide Mixtures by Computer Simulation and Intrinsic Surface Analysis; B. Kiss, B. Fábián, A. Idrissi, M. Szőri and P. Jedlovszky; *J. Phys. Chem. C* 2018, 122, 19639−19651; *DOI: 10.1021/acs.jpcc.8b05874*

3. Adsorption of Formamide at the Surface of Amorphous and Crystalline Ices under Interstellar and Tropospheric Conditions. A Grand Canonical Monte Carlo Simulation Study; B. Kiss, S. Picaud, M. Szőri and P. Jedlovszky; *J. Phys. Chem. A* 2019, 123, 2935−2948; *DOI: 10.1021/acs.jpca.9b00850*

Publications Not Included in The Thesis

1. Bioimprinted lipases in PVA nanofibers as efficient immobilized biocatalysts; D. Weiser, P. L. Sóti, G. Bánóczi, V. Bódai, B. Kiss, Á. Gellért, Z. K. Nagy, B. Koczka, A. Szilágyi, G. Marosi, L. Poppe; Tetrahedron 72 (2016) 7335-7342; *DOI: 10.1016/j.tet.2016.06.027*

2. Adsorption of Propylene Oxide on Amorphous Ice under Interstellar Conditions. A Grand Canonical Monte Carlo Simulation Study; B. Kiss, M. Szőri and P. Jedlovszky; *J. Phys. Chem. C* 2020, 124, 30, 16402–16414; *DOI: 10.1021/acs.jpcc.0c03722*

References

1. Oparin, A. I. *The Origin of Life*. (Macmillan, 1938).
2. Miller, S. L. A production of amino acids under possible primitive earth conditions. *Science (80-.).* **117**, 528–529 (1953).
3. Matthews, C. N. The HCN World. in *Origins* 121–135 (Kluwer Academic Publishers, 2006). doi:10.1007/1-4020-2522-x_8
4. Arrhenius, S. & Borns, H. Worlds in the Making. The Evolution of the Universe. *Bull. Am. Geogr. Soc.* **41**, 123 (1909).
5. Oró, J. Comets and the formation of biochemical compounds on the primitive earth. *Nature* **190**, 389–390 (1961).
6. Irvine, W. M. *et al.* The HNC/HCN ratio in comets. *Earth, Moon Planets* **78**, 29–35 (1997).
7. Rubin, R. H. *et al.* Microwave Detection of Interstellar Formamide. *Astrophys. J.* **169**, L39 (1971).
8. Adande, G. R., Woolf, N. J. & Ziurys, L. M. Observations of Interstellar Formamide: Availability of a Prebiotic Precursor in the Galactic Habitable Zone. *Astrobiology* **13**, 439–453 (2013).
9. Schutte, W. A. *et al.* Weak ice absorption features at 7.24 and 7.41 μm in the spectrum of the obscured young stellar object W 33A. *Astron. Astrophys.* **343**, 966–976 (1999).
10. Solomon, P. M. Interstellar molecules. *Phys. Today* **26**, 32–40 (1973).
11. Bockelée-Morvan, D. *et al.* New molecules found in comet C/1995 O1 (Hale-Bopp): Investigating the link between cometary and interstellar material. *Astron. Astrophys.* **353**, 1101–1114 (2000).
12. Carota, E., Botta, G., Rotelli, L., Di Mauro, E. & Saladino, R. Current Advances in Prebiotic Chemistry Under Space Conditions. *Curr. Org. Chem.* **19**, 1963–1979 (2015).
13. Ferus, M. *et al.* High-energy chemistry of formamide: A unified mechanism of nucleobase formation. *Proc. Natl. Acad. Sci.* **112**, 657–662 (2015).
14. Mispelaer, F. *et al.* Diffusion measurements of CO, HNCO, H 2 CO, and NH 3 in amorphous water ice. *Astron. Astrophys.* **555**, A13 (2013).
15. Cottin, H., Gazeau, M. C. & Raulin, F. Cometary organic chemistry: A review from observations, numerical and experimental simulations. *Planet. Space Sci.* **47**, 1141–1162 (1999).
16. Wakelam, V., Loison, J. C., Mereau, R. & Ruaud, M. Binding energies: New values and impact on the efficiency of chemical desorption. *Mol. Astrophys.* **6**, 22–35 (2017).
17. Tsuchida, E. Ab initio molecular-dynamics study of liquid formamide. *J. Chem. Phys.* **121**, 4740–4746 (2004).
18. Elola, M. D. & Ladanyi, B. M. Intermolecular polarizability dynamics of aqueous formamide liquid mixtures studied by molecular dynamics simulations. *J. Chem. Phys.* **126**, 084504 (2007).
19. Coutant, C., Properties, P., David E. Mears1, A. D. E., Fumagalli, C. & Fruscella, W. Kirk-Othmer Encyclopedia of Chemical Technology. *Kirk-Othmer Encycl. Chem. Technol.* **3**, 596–624 (2000).
20. Zaichikov, A. M.; Golubinskii, O. E. Enthalpy of Mixing of Water with Some Primer and Secunder Amides. *Zh. Fiz. Khim* **70**, 1175–1179 (1996).
21. Zaichikov, A. M. Thermochemical study of the ternary system water - formamide - dimethylacetamide. *Russ. J. Gen. Chem.* **71**, 162–167 (2001).
22. Zoranić, L., Mazighi, R., Sokolić, F. & Perera, A. Concentration fluctuations and microheterogeneity in aqueous amide mixtures. *J. Chem. Phys.* **130**, 124315 (2009).
23. Bakó, I. *et al.* Hydrogen bonded network properties in liquid formamide. *J. Chem. Phys.* **132**, 014506 (2010).
24. Bakó, I. *et al.* Water-formamide mixtures: Topology of the hydrogen-bonded network. *J. Mol. Liq.* **228**, 25–31 (2017).
25. Jedlovszky, P., Idrissi, A. & Jancsó, G. Can existing models qualitatively describe the mixing behavior of acetone with water? *J. Chem. Phys.* **130**, 124516 (2009).
26. Puhovski, Y. P. & Rode, B. M. Molecular dynamics simulations of aqueous formamide solution. II. Dynamics of solvent molecules. *J. Chem. Phys.* **102**, 2920–2927 (1995).
27. Howard, P. H. *Handbook of Environmental Fate and Exposure Data for Organic Chemicals, Volume IV*. (Lewis, 1993).

28. Stribling, R. & Miller, S. L. Energy yields for hydrogen cyanide and formaldehyde syntheses: The hcn and amino acid concentrations in the primitive ocean. *Orig. life Evol. Biosph.* **17**, 261–273 (1987).
29. Szori, M. & Jedlovszky, P. Adsorption of HCN at the surface of ice: A grand canonical Monte Carlo simulation study. *J. Phys. Chem. C* **118**, 3599–3609 (2014).
30. Fábián, B., Szöri, M. & Jedlovszky, P. Floating patches of HCN at the surface of their aqueous solutions - Can they make 'hCN World' plausible? *J. Phys. Chem. C* **118**, 21469–21482 (2014).
31. MEZEI, M. & BEVERIDGE, D. L. Free Energy Simulations. *Ann. N. Y. Acad. Sci.* **482**, 1–23 (1986).
32. Jorgensen, W. L. & Swenson, C. J. Optimized intermolecular potential functions for amides and peptides. Structure and properties of liquid amides. *J. Am. Chem. Soc.* **107**, 569–578 (1985).
33. Jorgensen, W. L., Maxwell, D. S. & Tirado-Rives, J. Development and testing of the OPLS all-atom force field on conformational energetics and properties of organic liquids. *J. Am. Chem. Soc.* **118**, 11225–11236 (1996).
34. De La Luz, A. P., Méndez-Maldonado, G. A., Núñez-Rojas, E., Bresme, F. & Alejandre, J. A New Force Field of Formamide and the Effect of the Dielectric Constant on Miscibility. *J. Chem. Theory Comput.* **11**, 2792–2800 (2015).
35. Lindahl, E., Bjelkmar, P., Larsson, P., Cuendet, M. A. & Hess, B. Implementation of the charmm force field in GROMACS: Analysis of protein stability effects from correction maps, virtual interaction sites, and water models. *J. Chem. Theory Comput.* **6**, 459–466 (2010).
36. Cordeiro, J. M. M. C — H ... O and N — H ...O Hydrogen Bonds in Liquid Amides Investigated by Monte Carlo Simulation. *Int. J. Quantum Chem.* **66**, 709–727 (1997).
37. Macchiagodena, M. *et al.* Accurate prediction of bulk properties in hydrogen bonded liquids: amides as case studies. *Phys. Chem. Chem. Phys.* **18**, 25342–25354 (2016).
38. Berendsen, H. J. C., Grigera, J. R. & Straatsma, T. P. The missing term in effective pair potentials. *J. Phys. Chem.* **91**, 6269–6271 (1987).
39. Jorgensen, W. L., Chandrasekhar, J., Madura, J. D., Impey, R. W. & Klein, M. L. Comparison of simple potential functions for simulating liquid water. *J. Chem. Phys.* **79**, 926–935 (1983).
40. Abascal, J. L. & Vega, C. A general purpose model for the condensed phases of water: TIP4P/2005. *J. Chem. Phys.* **123**, 234505 (2005).
41. Allen, M. P. & Tildesley, D. J. Computer simulation of liquids. *Oxford Univ. Press. New York* (1987). doi:10.2307/2938686
42. Pártay, L. B., Hantal, G., Jedlovszky, P., Vincze, Á. & Horvai, G. A new method for determining the interfacial molecules and characterizing the surface roughness in computer simulations. Application to the liquid-vapor interface of water. *J. Comput. Chem.* **29**, 945–956 (2008).
43. Vlllamañán, M. A. & Van Ness, H. C. Excess Thermodynamic Properties for Water/Acetone. *J. Chem. Eng. Data* **29**, 429–431 (1984).
44. Voronoi, G. F. Recherches sur le Paralléloèders Primitives. *J. Reine Angew. Math.* **134**, 198–287 (1908).
45. Fábián, B., Sega, M., Horvai, G. & Jedlovszky, P. Single Particle Dynamics at the Intrinsic Surface of Various Apolar, Aprotic Dipolar, and Hydrogen Bonding Liquids As Seen from Computer Simulations. *J. Phys. Chem. B* **121**, 5582–5594 (2017).
46. Zaninetti, L. The Voronoi tessellation generated from different distributions of seeds. *Phys. Lett. A* **165**, 143–147 (1992).
47. Kiss, B., Fábián, B., Idrissi, A., Szöri, M. & Jedlovszky, P. Miscibility and Thermodynamics of Mixing of Different Models of Formamide and Water in Computer Simulation. *J. Phys. Chem. B* **121**, 7147–7155 (2017).
48. Jedlovszky, P., Vincze, Á. & Horvai, G. New insight into the orientational order of water molecules at the water/1,2-dichloroethane interface: A Monte Carlo simulation study. *J. Chem. Phys.* **117**, 2271–2280 (2002).
49. Jedlovszky, P., Vincze, Á. & Horvai, G. Full description of the orientational statistics of molecules near to interfaces. Water at the interface with CCl4. in *Physical Chemistry Chemical Physics* **6**, 1874–1879 (2004).